

# A Minimal Dark $SU(2)$ Origin of a Massless Dirac Neutrino

P. S. Bhupal Dev,<sup>1,2</sup> Julia Gehrlein,<sup>3</sup> Amartya Sengupta,<sup>4,5</sup> and Amarjit Soni<sup>6</sup>

<sup>1</sup>*Department of Physics and McDonnell Center for the Space Sciences,  
Washington University, Saint Louis, Missouri 63130, USA*

<sup>2</sup>*PRISMA<sup>++</sup> Cluster of Excellence & Mainz Institute for Theoretical Physics,  
Johannes Gutenberg-Universität Mainz, 55099 Mainz, Germany*

<sup>3</sup>*Department of Physics, Colorado State University, Fort Collins, Colorado 80523, USA*

<sup>4</sup>*Department of Physics, The State University of New York, Buffalo, New York 14260, USA*

<sup>5</sup>*International Center for Quantum-field Measurement Systems for Studies of the Universe and Particles (QUP),  
KEK, 1-1 Oho, Tsukuba, Ibaraki 305-0801, Japan*

<sup>6</sup>*High Energy Theory Group, Physics Department,  
Brookhaven National Laboratory, Upton, New York 11973, USA*

We propose a gauge-symmetry origin of a rank-two Dirac neutrino mass matrix that enforces one exactly massless neutrino, while being consistent with the oscillation data, as well as cosmological constraints. The mechanism relies on a minimal dark  $SU(2)_D$  gauge symmetry under which one right-handed-neutrino-like Weyl fermion is charged, thereby forbidding its Standard Model Yukawa coupling. Quantum consistency then fixes the minimal dark-sector completion: Cancellation of the Witten anomaly requires a second fermionic  $SU(2)_D$  doublet, while a discrete  $Z_4$  symmetry that forbids Majorana masses allows the two dark doublets to form a vectorlike pair. This anomaly-free completion gives rise to a secluded, confining dark sector with a viable dark matter candidate, linking the protected neutrino texture to dark infrared dynamics.

## INTRODUCTION

The observation of neutrino oscillations [1, 2] has increased the number of free parameters in the Standard Model (SM) by at least seven: three mixing angles, three neutrino masses, and at least one CP phase. While neutrino oscillation experiments are making steady progress in measuring the oscillation parameters more precisely [3], with further improvements anticipated from ongoing and next-generation experiments like JUNO [4], IceCube/DeepCore [5], Hyper-Kamiokande [6], DUNE [7], and their combinations [8–12], none of the oscillation experiments are sensitive to the absolute neutrino mass scale. The observed solar and atmospheric mass-squared splittings require two non-zero neutrino masses, while the mass of the lightest neutrino cannot be constrained by oscillation experiments, and remains an open question. Instead, we have to rely on cosmological observations of large-scale structure, which constrain the sum of neutrino masses [13], and precise laboratory measurements of the endpoint of the beta-decay spectrum [14] to provide complementary information on the neutrino mass scale. The direct laboratory searches, while impressive, are currently far from the sensitivity required to probe even the inverted ordering (IO), let alone normal ordering (NO) [15]. Additional information on the neutrino masses can be obtained if a galactic supernova is detected [6, 16–26] or a measurement of the cosmic neutrino background is achieved [27, 28].

Currently, the strongest constraints on the neutrino mass scale come from the recent DESI BAO analysis [29]. When interpreted within the  $\Lambda$ CDM cosmology [30, 31], it places an upper bound on the sum of neutrino masses

$\sum_i m_i < 64$  meV (95% CL). Slightly weaker constraints are obtained from Planck [30], ACT [32] and SPT [33] datasets, while a combination of ACT+SPT+Planck gives a slightly stronger bound  $\sum_i m_i < 62$  meV (95% CL) [34]. These upper bounds are close to the minimum value of  $\sum m_i$  allowed by oscillation data for NO, and already in tension with the corresponding value for IO. Any emerging tension with NO can be alleviated if the lightest neutrino is (nearly) massless. Although this conclusion might change depending on the assumed cosmological model [35–51] and the presence of additional neutrino interactions [52–57], the increasing precision of cosmological constraints provide a timely motivation to consider theories in which the lightest neutrino remains exactly massless.<sup>1</sup>

Existing models with one massless neutrino rely on a minimal field content of just two right-handed neutrinos instead of the three needed to generate masses for all SM neutrinos. Popular ones include the minimal scotogenic model [60–63], minimal type-I seesaw [64–67] constructions with two right-handed-neutrinos [68–76], and variants of the type-I seesaw such as inverse seesaw [77]-based minimal models [78–82]. These models are phenomenologically viable, although if one tries to gauge the usual  $B - L$  symmetry with only two ordinary right-handed neutrinos, additional chiral states or non-standard charge assignments are required for anomaly cancellation. This prevents these models from featuring an additional gauged  $B - L$  symmetry, which is desirable to protect the neutrino mass, and also for generat-

<sup>1</sup> Additional theoretical motivation for a massless neutrino comes from models with a CPT-symmetric universe [58, 59].

ing a massive gauge boson after lepton-number breaking associated with Majorana mass terms, or embedding it within grand unified theories where  $B - L$  is part of a bigger gauge group. An alternative approach is to postulate a texture of the neutrino mass matrix which leads to only two non-zero eigenvalues [83–86]. However, in this case the zero neutrino mass is in general not protected from higher order corrections, rendering it non-zero at a certain energy scale [87], although in some models the texture zeros are stable [88, 89].

Here, we instead show that a massless neutrino can follow from a gauge selection rule. Due to its symmetry origin, the zero neutrino mass is protected from corrections and one neutrino remains massless at all energy scales and all orders in perturbation theory. As a minimal example, we introduce a  $SU(2)_D$  gauge symmetry under which one right-handed-neutrino-like SM singlet Weyl fermion  $N_1$  transforms as a doublet. Furthermore, quantum consistency constrains the additional dark fermion content, which can accommodate a dark matter (DM) candidate, as shown below.<sup>2</sup>

### THE MINIMAL MODEL

The minimal choice of the dark gauge group is  $SU(2)_D$  which features three massless dark gauge fields which couple to the fermions charged under this group with coupling strength  $g_D$ . To obtain an anomaly-safe dark gauge theory, the global Witten anomaly needs to be prevented which requires the introduction of an even number of  $SU(2)_D$  doublets [92]. Therefore, we include in addition to  $N_1$ , another  $SU(2)_D$  doublet Weyl-fermion field  $\xi$ . The SM fields and two right-handed neutrinos  $N_2, N_3$  are singlets under the dark gauge group. All new fermions are singlets under the SM gauge groups. Additionally, we impose a discrete  $Z_4$  symmetry, acting on the SM fermions and on the new singlet and dark-sector fermions, to keep the neutrino sector Dirac. The masslessness of one neutrino is enforced by the dark gauge charge, which forbids one Dirac Yukawa column. However, the dark gauge symmetry alone does not exclude Majorana-type bilinears for the SM-singlet fermions; if present, these terms would turn the model into a Majorana or seesaw-like construction rather than a rank-two Dirac-neutrino model. The chosen  $Z_4$  assignment allows the charged-lepton and Dirac-neutrino Yukawa terms,

Field	$SU(3)_c \times SU(2)_L \times U(1)_Y$	$SU(2)_D$	$Z_4$
$L_i$	$(\mathbf{1}, \mathbf{2}, -1/2)$	$\mathbf{1}$	1
$e_{Ri}$	$(\mathbf{1}, \mathbf{1}, -1)$	$\mathbf{1}$	1
$H$	$(\mathbf{1}, \mathbf{2}, 1/2)$	$\mathbf{1}$	0
$N_1$	$(\mathbf{1}, \mathbf{1}, 0)$	$\mathbf{2}$	1
$\xi$	$(\mathbf{1}, \mathbf{1}, 0)$	$\mathbf{2}$	3
$N_2, N_3$	$(\mathbf{1}, \mathbf{1}, 0)$	$\mathbf{1}$	1

TABLE I. SM lepton and Higgs, and dark-sector fermion charges under  $SU(2)_D$  and  $Z_4$ .

forbids Majorana masses, but permits the mixed dark bilinear involving  $N_1$  and  $\xi$ . A  $Z_2$  symmetry acting on the same fermions would not be sufficient, since the Majorana bilinears would be even under it. The field content and their charges are shown in Table I.

With these charge assignments, the allowed renormalizable Yukawa interactions with the SM lepton and Higgs sector are

$$\mathcal{L}_Y = -(Y_e)_{ij} \bar{L}_i H e_{Rj} - (Y_\nu)_{i\alpha} \bar{L}_i \tilde{H} N_\alpha + \text{H.c.}, \quad (1)$$

where  $\tilde{H} = i\sigma_2 H^*$ ;  $i, j = 1, 2, 3$ , and  $\alpha = 2, 3$ . The Majorana-type operators

$$N_\alpha N_\beta, \quad \epsilon_{ab} N_1^a N_1^b, \quad \epsilon_{ab} \xi^a \xi^b \quad (2)$$

carry charge 2 modulo four and are therefore absent in the  $Z_4$ -symmetric theory. Here  $\epsilon_{ab}$ , with  $\epsilon_{12} = +1$ , denotes the antisymmetric  $SU(2)_D$ -invariant tensor used to contract two dark-doublet indices. The mixed dark bilinear  $\epsilon_{ab} N_1^a \xi^b$  has charge  $1 + 3 = 4 = 0 \pmod{4}$ , so the vectorlike mass

$$\mathcal{L}_{\text{mass}} = -m_D \epsilon_{ab} N_1^a \xi^b + \text{H.c.} \quad (3)$$

is allowed and it controls the dark infrared dynamics which feature a confinement scale  $\Lambda_D$ . For  $m_D \gg \Lambda_D$ , the dark doublets decouple and the low-energy theory approaches pure  $SU(2)_D$  Yang–Mills; for  $m_D \lesssim \Lambda_D$ , the dark fermions remain part of the confined spectrum. The corresponding dark-sector phenomenology depends on this hierarchy, as discussed later.

### MINIMALITY AND ALTERNATIVE CHOICES OF THE DARK SYMMETRY

The zero-column mechanism itself does not require a non-Abelian group; an Abelian dark charge could also forbid  $\bar{L}_i \tilde{H} N_1$ . We choose a non-Abelian realization because it also produces a secluded confining sector with an infrared scale generated by strong dynamics. With this added requirement,  $SU(2)_D$  is the smallest possible choice. Its minimal consistency issue is the Witten anomaly, already removed by the second doublet  $\xi$  introduced above.

<sup>2</sup>  $SU(2)_D$  in the context of Dirac neutrino mass and DM has also been considered in Ref. [90, 91], where the  $SU(2)_D$  gauge symmetry is spontaneously broken to retain a global  $SU(2)$  symmetry. Two Dirac neutrino masses are generated at one loop from the  $SU(2)_D$  dark fermions and scalars. In our mechanism, the  $SU(2)_D$  gauge symmetry remains unbroken and Dirac neutrino masses arise at tree level.

A hidden  $SU(3)_D$  theory is a natural alternative. It is similar to QCD and can support dark baryons. But a single Weyl fundamental of  $SU(3)_D$  is perturbatively anomalous. The smallest anomaly-free version introduces an antifundamental partner,  $\psi_D \sim \mathbf{3}, \eta_D \sim \bar{\mathbf{3}}$ , making the dark sector vectorlike. Such models may be preferable for dark baryon stability or first-order confinement, but they are less minimal to predict a massless neutrino. Other non-Abelian groups like  $SO(N \geq 4)$  and  $Sp(N \geq 2)$  can also realize the zero-column mechanism, but their spectra and accidental symmetries differ from the minimal  $SU(2)_D$  case.

### NEUTRINO MASS MATRIX

After electroweak symmetry breaking, the Lagrangian (1) generates a Dirac neutrino mass matrix

$$M_\nu = \frac{v}{\sqrt{2}} Y_\nu, \quad Y_\nu = \begin{pmatrix} 0 & y_{12} & y_{13} \\ 0 & y_{22} & y_{23} \\ 0 & y_{32} & y_{33} \end{pmatrix}, \quad (4)$$

where  $v$  is the electroweak vacuum expectation value. The first column of  $Y_\nu$  is identically zero because  $N_1$  has a dark gauge charge which does not allow its coupling to the SM neutrinos. We nevertheless display the texture in a  $3 \times 3$  square form by reserving the first column for the dark-charged state  $N_1$ . Hence  $\det M_\nu = 0$ , and one physical Dirac neutrino mass vanishes. Working in the charged-lepton mass basis, the Dirac mass matrix is diagonalized by

$$U_{\text{PMNS}}^\dagger M_\nu U_R = \text{diag}(m_1, m_2, m_3), \quad (5)$$

where  $U_R$  is an arbitrary unitary matrix diagonalizing the  $N_i$  sector and  $U_{\text{PMNS}}$  is the measurable PMNS mixing matrix [93, 94]. Furthermore, since  $N_2$  and  $N_3$  carry identical charges, we can perform a right-handed  $U(2)$  rotation among them:<sup>3</sup>

$$\begin{pmatrix} N_2 \\ N_3 \end{pmatrix} \rightarrow R \begin{pmatrix} N_2 \\ N_3 \end{pmatrix}, \quad R \in U(2). \quad (6)$$

Let  $B$  be the  $3 \times 2$  matrix formed by the nonzero columns of  $M_\nu$ . If the second row of  $B$  is  $(w_1, w_2)$ , choose

$$R^\dagger = \frac{1}{\sqrt{|w_1|^2 + |w_2|^2}} \begin{pmatrix} w_2 & w_1^* \\ -w_1 & w_2^* \end{pmatrix}. \quad (7)$$

Then the second-row entry of the rotated two-column block vanishes, and the full matrix can be written as

$$M_\nu = \begin{pmatrix} 0 & m_{12} & m_{13} \\ 0 & 0 & m_{23} \\ 0 & m_{32} & m_{33} \end{pmatrix}. \quad (8)$$

This is the  $D_{76}$  class of four-zero texture Dirac mass matrix [86].<sup>4</sup> In the present model this is a basis representation, not an additional flavor prediction; the invariant statement is one gauge-protected zero column. Since the two nonzero columns correspond to fields with identical charges, the additional zero can equivalently be placed in another entry of the second or third column by an appropriate right-handed  $U(2)$  basis choice. These choices correspond to other  $D$ -type textures with one zero column in the texture-zero classification, but only  $D_{76}$  in Eq. (8) and the electron-row representative  $D_{16}$  (with  $m_{12} = 0$ ) are compatible with the current oscillation data for both NO and IO [86]. We focus on  $D_{76}$  because the physical zero  $(M_\nu)_{\mu 2} = 0$  involves  $\mu$ -row PMNS elements which depend on both  $\theta_{23}$  and  $\delta_{\text{CP}}$ :  $U_{\mu 2}, U_{\mu 3}$  for NO and  $U_{\mu 1}, U_{\mu 2}$  for IO, and can therefore correlate  $\theta_{23}$  with  $\delta_{\text{CP}}$  once the right-handed basis is fixed by additional flavor structure (see Appendix).

### PHENOMENOLOGY

#### Neutrino sector

As stated before, we predict a zero lightest neutrino mass in this model. The other neutrino masses are fixed by the measured mass splittings  $\Delta m_{21}^2$  and  $\Delta m_{31}^2$ :

$$\begin{aligned} \text{NO} : m_1 = 0, \quad m_2 = \sqrt{\Delta m_{21}^2}, \quad m_3 = \sqrt{\Delta m_{31}^2}, \\ \text{IO} : m_3 = 0, \quad m_1 = \sqrt{|\Delta m_{31}^2|}, \quad m_2 = \sqrt{|\Delta m_{31}^2| + \Delta m_{21}^2}. \end{aligned} \quad (9)$$

The observable related to the end point of the beta decay spectrum is [15]

$$m_\beta^2 = \sum_i |U_{ei}|^2 m_i^2, \quad (10)$$

with  $U_{ei}$  the PMNS matrix elements in the electron row. Using the recent JUNO results for the solar sector [97], together with the NuFIT 6.0 best-fit values for the remaining oscillation parameters [98], we find for Eq. (10) and the sum of the neutrino masses:

$$\begin{aligned} \text{NO} : m_\beta = 8.85_{-0.57}^{+0.59} \text{ meV}, \quad \sum_i m_i = 58.79_{-1.04}^{+1.07} \text{ meV}, \\ \text{IO} : m_\beta = 48.76_{-0.88}^{+1.08} \text{ meV}, \quad \sum_i m_i = 98.92_{-1.65}^{+2.06} \text{ meV}, \end{aligned} \quad (11)$$

<sup>3</sup> This freedom of choosing basis in the  $(N_2, N_3)$  space follows solely from the identical quantum numbers of  $N_2$  and  $N_3$ , and is independent of the particular choice of dark symmetry group.

<sup>4</sup> Four-zero texture neutrino masses have been discussed in Ref. [95]. An  $SO(10)$  GUT embedding of related texture-zero structures has been studied in Ref. [96].

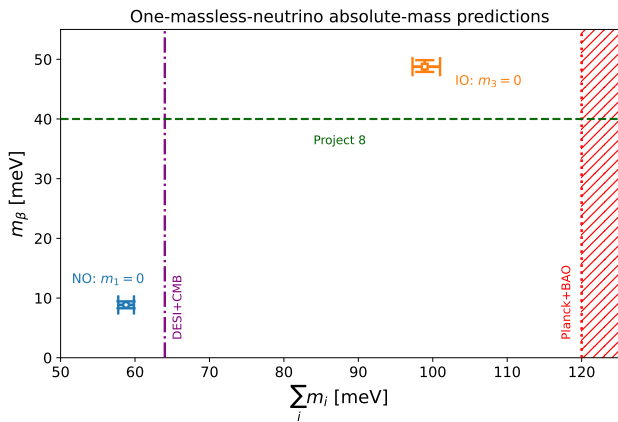


FIG. 1. Absolute-mass predictions for the zero-column representative texture with one massless Dirac neutrino. Error bars show the propagated uncertainties obtained by scanning representative  $3\sigma$  oscillation-parameter ranges in both  $\sum_i m_i$  and  $m_\beta$ . The vertical lines indicate the DESI+CMB [29] and Planck+BAO [30]  $\Lambda$ CDM reference bounds on  $\sum_i m_i$ , and the green dashed line shows the approximate Project 8 target sensitivity near  $m_\beta \simeq 40$  meV [99]. The current KATRIN bound on  $m_\beta$  lies above the plotted range [15].

where the error bars account for the  $3\sigma$  oscillation-parameter uncertainties (see Fig. 1). The predicted values of  $m_\beta$  are far below the current KATRIN bound,  $m_\beta < 450$  meV [15]. For the sum of neutrino masses, the NO prediction lies below both the standard Planck+BAO  $\Lambda$ CDM bound  $\sum_i m_i < 120$  meV [30] and the stronger DESI+CMB  $\Lambda$ CDM bound  $\sum_i m_i < 64$  meV [29]. The IO prediction remains allowed by Planck+BAO but disfavored by DESI+CMB.

Future improvements in direct beta-decay searches from experiments like KATRIN [100], ECHO [101], HOLMES [102] and Project 8 [99] could eventually reach sensitivities down to  $m_\beta \simeq 40$  meV and probe the IO case, while the NO prediction is more challenging to reach. Future CMB and large-scale-structure surveys can further test the mass-sum prediction, with CMB-S4+DESI-like combinations expected to reach  $\mathcal{O}(10$  meV) precision in representative forecasts [103–106]. This would directly probe the NO prediction near 59 meV. Figure 1 summarizes the relevant absolute-mass probes.

This model features Dirac neutrinos which additionally predicts that neutrinoless double beta decay should not be observed. Also, the relic neutrino capture rate is smaller by a factor of two compared to the Majorana case, giving about 4.06 events/year for a 100 g PTOLEMY-like detector [107]. For a detector with an arbitrarily good energy resolution, each mass eigenstate  $\nu_i$  would make a distinguishable contribution to the  $C\nu\beta$  capture and to the beta decay spectrum. The beta decay spectrum would be the sum of three spectra, and its endpoint would

be determined by the lightest neutrino mass, which offers a way to test whether the lightest mass is zero or not. But in practice, the primary target energy resolution of PTOLEMY is  $\sim 50$  meV [27], so experimentally, it will be extremely difficult, if not impossible, to determine whether the lightest neutrino is exactly massless or has a nonzero mass smaller than the detector resolution.

## Dark sector

The neutrino results derived in the previous subsection do not require knowledge of the detailed spectrum of the dark gauge theory; instead, it follows from the non-trivial dark charge of only  $N_1$ . The dark-sector phenomenology however, depends on the choice of the gauge group and the particle spectrum.

Once  $SU(2)_D$  is gauged, the theory becomes strong in the infrared and generates its own mass scale by dimensional transmutation [108, 109]:

$$\Lambda_D = \mu \exp \left[ -\frac{8\pi^2}{b_0 g_D^2(\mu)} \right]. \quad (12)$$

Here  $b_0$  is the one-loop beta-function coefficient. With  $n_W$  Weyl fermion doublets and  $n_S$  complex scalar doublets of  $SU(2)_D$ ,

$$b_0 = \frac{22}{3} - \frac{n_W}{3} - \frac{n_S}{6}. \quad (13)$$

In the minimal model  $n_W = 2$  and  $n_S = 0$ , so  $b_0 = 20/3 > 0$ ; the dark gauge theory is therefore asymptotically free and is expected to confine in the infrared.<sup>5</sup>

As in QCD, a gauge theory with no elementary mass scale in the gauge sector can produce massive bound states after confinement. If the lightest confined states are stable or sufficiently long-lived, the particles in such a secluded confining sector provide natural DM candidates [110–122].

The confined spectrum depends on the hierarchy between  $m_D$ , the mass of the dark fermions, and the confinement scale  $\Lambda_D$ . If  $m_D \gg \Lambda_D$ , the dark doublets are heavy compared to the confinement scale, and the low-energy theory is close to pure Yang–Mills. The lightest states are then dark glueballs. The lightest scalar and pseudoscalar states may be written schematically in terms of the dark field-strength tensor  $G_{\mu\nu}^A$  and its dual  $\tilde{G}^{A\mu\nu}$  as

$$S_D \sim G_{\mu\nu}^A G^{A\mu\nu}, \quad P_D \sim G_{\mu\nu}^A \tilde{G}^{A\mu\nu}, \quad (14)$$

<sup>5</sup> Losing asymptotic freedom at one loop would require  $2n_W + n_S \geq 44$ , which gives  $n_W \geq 22$  Weyl doublets in the absence of scalar doublets.

where  $A = 1, 2, 3$  is the adjoint  $SU(2)_D$  gauge index. Their masses are of order

$$m_{S_D}, m_{P_D} \sim \kappa \Lambda_D, \quad (15)$$

where  $\kappa$  denotes nonperturbative coefficients derived from lattice studies of confining Yang–Mills spectra [123, 124]. If instead  $m_D \lesssim \Lambda_D$ , the dark doublets participate in the confined spectrum. The theory can then contain fermionic and bosonic dark hadrons built from  $N_1$  and  $\xi$ ; for example, states like

$$\epsilon_{ab} N_1^a \xi^b, \quad N_1^\dagger \bar{\sigma}^\mu \xi \quad (16)$$

arise, where  $\bar{\sigma}^\mu = (1, -\vec{\sigma})$  in two-component Weyl notation and  $\vec{\sigma}$  are the Pauli matrices. The detailed spectrum is nonperturbative, but the existence of a secluded confining sector follows directly from the anomaly-safe completion.

Whether the lightest confined state is a viable DM candidate depends on its stability. In the pure Yang–Mills limit,  $m_D \gg \Lambda_D$ , the lightest dark glueball is stable if no portal to the SM is present, and becomes long-lived when its decay proceeds only through higher-dimensional Higgs–dark-gluon operators. If  $m_D \lesssim \Lambda_D$ , the lightest dark hadron may instead contain the dark fermions  $N_1, \xi$ . Its stability then depends on the accidental global symmetries of the renormalizable dark-sector Lagrangian. In particular, the gauge interactions and the vectorlike mass term can preserve a dark fermion number, analogous to baryon number in QCD, even if this symmetry is not imposed explicitly. Higher-dimensional portal operators or additional ultraviolet (UV) interactions may violate this accidental symmetry and determine the lifetime of the lightest dark hadron.

The leading interactions of the dark sector with the SM arise through higher-dimensional portals. Since the dark gauge group is non-Abelian, there is no dimension-four kinetic mixing with hypercharge. The dark gauge theory can, however, contain its own topological term:

$$\mathcal{L}_{\theta_D} = \frac{\theta_D g_D^2}{32\pi^2} G_{\mu\nu}^A \tilde{G}^{A\mu\nu}, \quad \tilde{G}^{A\mu\nu} = \frac{1}{2} \epsilon^{\mu\nu\rho\sigma} G_{\rho\sigma}^A. \quad (17)$$

This term is internal to the dark sector and is not a portal to the SM. Its physical meaning depends on the dark-fermion mass structure. In the chiral limit, when an anomalous axial rotation of the dark fermions is available,  $\theta_D$  can be rotated away. For nonzero  $m_D$ , the physical CP-odd parameter is the dark analogue of  $\bar{\theta}$ , schematically  $\bar{\theta}_D = \theta_D + \arg m_D$ , up to convention-dependent signs.<sup>6</sup> It may affect dark CP violation, the confined

spectrum, or the finite-temperature transition, but it does not by itself lead to visible-sector interactions. The simplest Higgs portals involving dark gauge fields appear at dimension six:

$$\frac{c_G}{\Lambda^2} (H^\dagger H) G_{\mu\nu}^A G^{A\mu\nu}, \quad \frac{\tilde{c}_G}{\Lambda^2} (H^\dagger H) G_{\mu\nu}^A \tilde{G}^{A\mu\nu}. \quad (18)$$

Compact objects may also constrain parts of the dark-sector parameter space, although the resulting bounds are necessarily model-dependent. Neutron stars can gravitationally focus DM from their environments [128–131], but focusing alone does not imply capture: An incoming dark particle must lose energy through scattering, dark self-interactions, or another dissipative process in order to become bound. In the present model such interactions can arise from the Higgs–dark-gluon portal operators in Eq. (18), as well as from the confined dark dynamics itself.

If the DM is made of bosonic glueballs and is captured efficiently, its behavior inside the star can differ substantially from that of ordinary nuclear matter. The characteristic glueball size is set by the confinement scale,

$$R_D \sim \Lambda_D^{-1} \simeq 2 \times 10^{-14} \text{ cm} \left( \frac{1 \text{ GeV}}{\Lambda_D} \right). \quad (19)$$

For  $\Lambda_D \sim \text{GeV}$ , the bound states are microscopic and carry internal momenta of order a GeV, larger than the typical neutron Fermi momenta in neutron-star interiors. Moreover, glueballs are bosons and are not supported by Fermi pressure. Once captured and thermalized, a sufficiently large population may therefore settle near the stellar center and form a Bose condensate. Efficient annihilation of DM may heat up the neutron star, offering a potential probe in JWST observations of old neutron stars [132–134].

A genuine neutron-star constraint requires the full sequence of capture, thermalization, condensation, and possible gravitational collapse and black-hole growth [132, 135–138]. For a non-self-interacting boson of mass  $m_{\text{DM}}$ , the characteristic collapse number scales as  $N_{\text{crit}} \sim M_{\text{Pl}}^2/m_{\text{DM}}^2$ . Old neutron stars can therefore exclude part of the parameter space only if capture and thermalization are efficient, and if any black hole formed grows faster than it evaporates. The relevant rates depend on the portal scale  $\Lambda$ , the confinement scale  $\Lambda_D$ , and the nonperturbative matrix elements controlling glueball interactions. In the minimal model  $\Lambda$  is not fixed by the neutrino texture; it parametrizes whatever UV physics generates the higher-dimensional Higgs–gluon operators in Eq. (18). Thus neutron-star bounds can be powerful, but they require a dedicated analysis of the portal strength, capture, thermalization, and collapse conditions. We leave this dark-sector phenomenology for future work.

Finally, the dark confinement transition occurs at a temperature of order  $T_D \sim \Lambda_D$ . For the minimal

<sup>6</sup> In our model with vectorlike fermions,  $\bar{\theta}_D$  is physical, unlike in  $SU(2)_L$  of the SM, where due to the chiral nature of fermions, the electroweak  $\theta$ -parameter can be rotated away [125–127].

$SU(2)_D$  theory, one should not assume that the transition is strongly first order. Pure  $SU(2)$  Yang–Mills has a second-order deconfinement transition in the three-dimensional Ising universality class [139, 140], and light dark-sector can further change the thermal history, depending on other details such as the reheating temperature. Other theories, such as larger  $SU(N)_D$  groups or deformed dark sectors, may instead have first-order transitions. In such cases the same dark gauge framework can produce a stochastic gravitational-wave background [141–143]. Precise predictions on the phase transition and the potential resulting gravitational waves require a finite-temperature analysis of the dark theory which is left for future work.

## CONCLUSIONS

We have proposed a minimal dark  $SU(2)$  model where the lightest neutrino mass is exactly zero and is protected by gauge symmetry. We derived the phenomenological predictions in the neutrino sector for this model and showed that it can be probed with future improvements in direct beta-decay searches and cosmological neutrino mass measurements. The neutrino mass matrix has a four-zero texture that could also be tested in future oscillation experiments. Beyond the neutrino texture, the same anomaly-safe completion leads to a secluded confining sector with a potential DM candidate, and depending on the model parameters, may provide a promising target for dark sector phenomenology using gravitational-wave and compact-object studies.

## ACKNOWLEDGMENTS

We thank George Parker and Robert Szafron for useful discussions and comments on the draft. We also thank Sharon Adler and Shaouly Bar-Shalom for encouragement that helped bring this work to completion. The work of BD is partly supported by the U.S. Department of Energy under grant No. DE-SC0017987 and by a Humboldt Fellowship from the Alexander von Humboldt Foundation. AS is partially supported by the NSF Grant No. PHY-2310363 and by a QUP internship.

## APPENDIX:

### FLAVOR COMPLETION OF THE $D_{76}$ TEXTURE

We follow the standard non-Hermitian Dirac mass matrix texture-zero notation of Ref. [86]. In the minimal model, the  $D_{76}$  form is simply a basis representation of the gauge-protected zero-column matrix. The physical prediction of the minimal construction is one exactly massless neutrino. Additional flavor structure fixing the

$(N_2, N_3)$  basis can make the  $D_{76}$  texture predictive for other observables (see e.g., Refs. [144–147]).

In the diagonal charged-lepton mass basis [cf. Eq. (5)],

$$M_\nu = U_{\text{PMNS}} D_\nu U_R^\dagger, \quad D_\nu = \text{diag}(m_1, m_2, m_3), \quad (\text{A1})$$

so that

$$(M_\nu)_{\alpha\beta} = \sum_{i=1}^3 m_i U_{\alpha i} (U_R)_{\beta i}^*, \quad \alpha = e, \mu, \tau. \quad (\text{A2})$$

The dark gauge symmetry enforces

$$(M_\nu)_{\alpha 1} = 0 \quad (\alpha = e, \mu, \tau). \quad (\text{A3})$$

Using Eq. (A2) and the unitarity of  $U_{\text{PMNS}}$ , this implies

$$m_i (U_R)_{1i}^* = 0 \quad (i = 1, 2, 3). \quad (\text{A4})$$

Thus the forbidden right-handed direction is aligned with the massless state. For NO,

$$(U_R)_{1i} = (e^{i\alpha_1}, 0, 0), \quad (\text{A5})$$

whereas for IO,

$$(U_R)_{1i} = (0, 0, e^{i\alpha_1}). \quad (\text{A6})$$

Consider the  $D_{76}$  representative texture with the additional zero [cf. Eq. (8)]

$$(M_\nu)_{\mu 2} = 0. \quad (\text{A7})$$

For NO, the second right-handed direction lies in the massive (2, 3) subspace and may be written as

$$(U_R)_{2i} = (0, \cos \theta_R, e^{i\phi_R} \sin \theta_R), \quad (\text{A8})$$

up to irrelevant phases. Here  $\theta_R$  and  $\phi_R$  parameterize the mixing angle and relative phase in the right-handed  $(N_2, N_3)$  subspace, respectively. The zero condition gives

$$m_2 U_{\mu 2} \cos \theta_R + m_3 U_{\mu 3} e^{-i\phi_R} \sin \theta_R = 0. \quad (\text{A9})$$

Using

$$U_{\mu 2} = c_{12} c_{23} - s_{12} s_{23} s_{13} e^{i\delta_{\text{CP}}}, \quad U_{\mu 3} = s_{23} c_{13}, \quad (\text{A10})$$

where  $s_{ij} \equiv \sin \theta_{ij}$ ,  $c_{ij} \equiv \cos \theta_{ij}$ , and  $\delta_{\text{CP}}$  is the Dirac CP phase in the PMNS matrix, the modulus condition gives

$$\tan \theta_R^{\text{NO}} = \frac{m_2 |U_{\mu 2}|}{m_3 |U_{\mu 3}|}. \quad (\text{A11})$$

For IO, the second right-handed direction lies in the massive (1, 2) subspace,

$$(U_R)_{2i} = (\cos \theta_R, e^{i\phi_R} \sin \theta_R, 0), \quad (\text{A12})$$

and the zero condition gives

$$m_1 U_{\mu 1} \cos \theta_R + m_2 U_{\mu 2} e^{-i\phi_R} \sin \theta_R = 0, \quad (\text{A13})$$

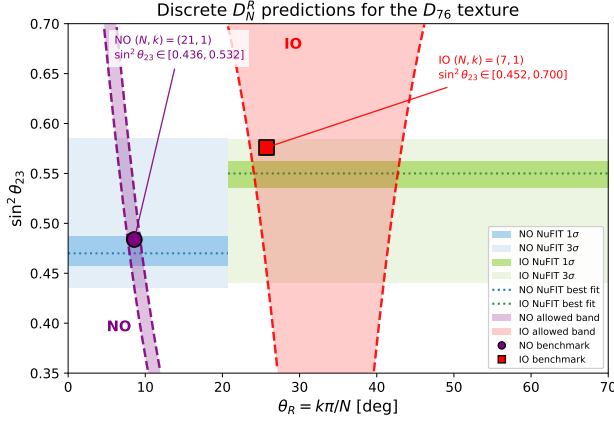


FIG. A1. Predicted intervals for the  $D_{76}$  representative four-zero texture Dirac neutrino mass matrix in a right-handed dihedral flavor completion. The right-handed angle is fixed as  $\theta_R = k\pi/N$ . The purple shaded region denotes the NO predicted band, while the red shaded region denotes the IO predicted band; the dashed boundaries show the corresponding edges of the predicted regions after marginalizing over  $\delta_{CP}$ . The blue bands on the NO side show the NuFIT  $1\sigma$  and  $3\sigma$  allowed regions for  $\sin^2 \theta_{23}$ , while the green bands on the IO side show the corresponding IO NuFIT regions [98]. The dotted horizontal lines indicate the NO and IO NuFIT best-fit values. The highlighted benchmarks  $(N, k) = (21, 1)$  for NO and  $(N, k) = (7, 1)$  for IO are used as representative choices for the fixed flavor+CP correlation plots in Fig. A3.

with

$$U_{\mu 1} = -s_{12}c_{23} - c_{12}s_{23}s_{13}e^{i\delta_{CP}}. \quad (\text{A14})$$

Taking the modulus gives

$$\tan \theta_R^{\text{IO}} = \frac{m_1}{m_2} \frac{|U_{\mu 1}|}{|U_{\mu 2}|}. \quad (\text{A15})$$

In the minimal zero-column model, Eqs. (A11) and (A15) are not constraints. They become predictions only after a flavor symmetry fixes the right-handed direction.

As an illustration, we take a right-handed dihedral symmetry  $D_N^R$ , where  $D_N$  denotes the symmetry group of a regular  $N$ -gon,<sup>7</sup> with  $(N_2, N_3)$  transforming as a doublet. If  $D_N^R$  is broken to a residual reflection, the direction in the  $(N_2, N_3)$  plane is fixed to

$$\theta_R = \frac{k\pi}{N}, \quad k = 1, \dots, N-1. \quad (\text{A16})$$

For each such discrete value of  $\theta_R$ , Eqs. (A11) and (A15) select an allowed interval in  $\sin^2 \theta_{23}$ , after marginalizing over  $\delta_{CP}$ , as shown in Fig. A1.

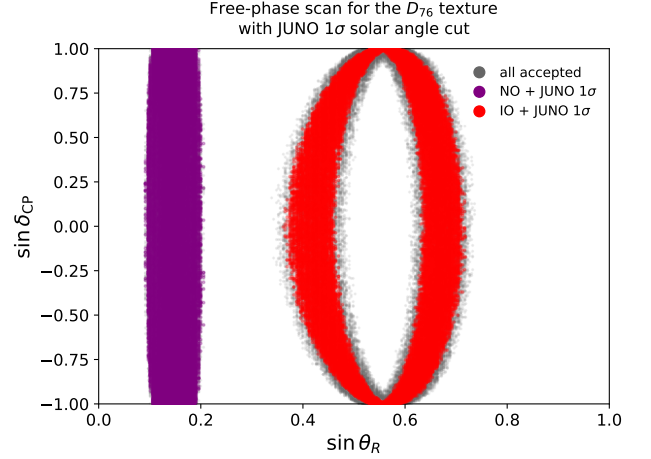


FIG. A2. Illustrative right-handed flavor completion with a physical  $\mu$ -row  $D$ -type zero texture ( $D_{76}$ ). The scan is shown in the  $(\sin \theta_R, \sin \delta_{CP})$  plane with a free right-handed phase  $\phi_R$ . Gray points satisfy the  $D_{76}$ -type zero condition within numerical tolerance, while purple and red points additionally satisfy the JUNO  $1\sigma$  solar-angle constraint for NO and IO, respectively.

For the numerical illustration in Fig. A1, we use the NuFIT 6.0 [98] oscillation parameter values. The highlighted choices  $(N, k) = (21, 1)$  for NO and  $(N, k) = (7, 1)$  for IO are used below as representative fixed flavor-completion benchmarks.

Since  $N_2$  and  $N_3$  have identical gauge and  $Z_4$  charges, a right-handed  $U(2)$  rotation can move the additional zero to another entry of the second or third column without violating any symmetry of the minimal model. In the minimal theory this remains a basis choice; it becomes physical only after additional flavor structure fixes the  $(N_2, N_3)$  basis. A  $\mu$ -row representative texture then gives a genuine atmospheric-angle–CP-phase correlation. In Fig. A2, we show an illustrative scan with free  $\phi_R$ , imposing the zero by matching the magnitudes of the two terms in Eq. (A9). Here, we also include the JUNO first-result values for the solar oscillation parameters [97]

$$\begin{aligned} \sin^2 \theta_{12} &= 0.3092 \pm 0.0087, \\ \Delta m_{21}^2 &= (7.50 \pm 0.12) \times 10^{-5} \text{ eV}^2, \end{aligned} \quad (\text{A17})$$

together with the remaining oscillation inputs from NuFIT [98] to show the impact of the JUNO results on this texture.

If the flavor completion fixes not only  $\theta_R$  but also the right-handed phase  $\phi_R$ , the  $D_{76}$  condition gives sharper correlations in the  $(\sin^2 \theta_{23}, \delta_{CP})$  plane. In Fig. A3, we use the representative choices selected from Fig. A1:

$$\begin{aligned} \text{NO} : \theta_R &= \frac{\pi}{21}, & \phi_R &= \pi, \\ \text{IO} : \theta_R &= \frac{\pi}{7}, & \phi_R &= \frac{\pi}{14}. \end{aligned} \quad (\text{A18})$$

<sup>7</sup> Some conventions use a group label differing by a factor of two.

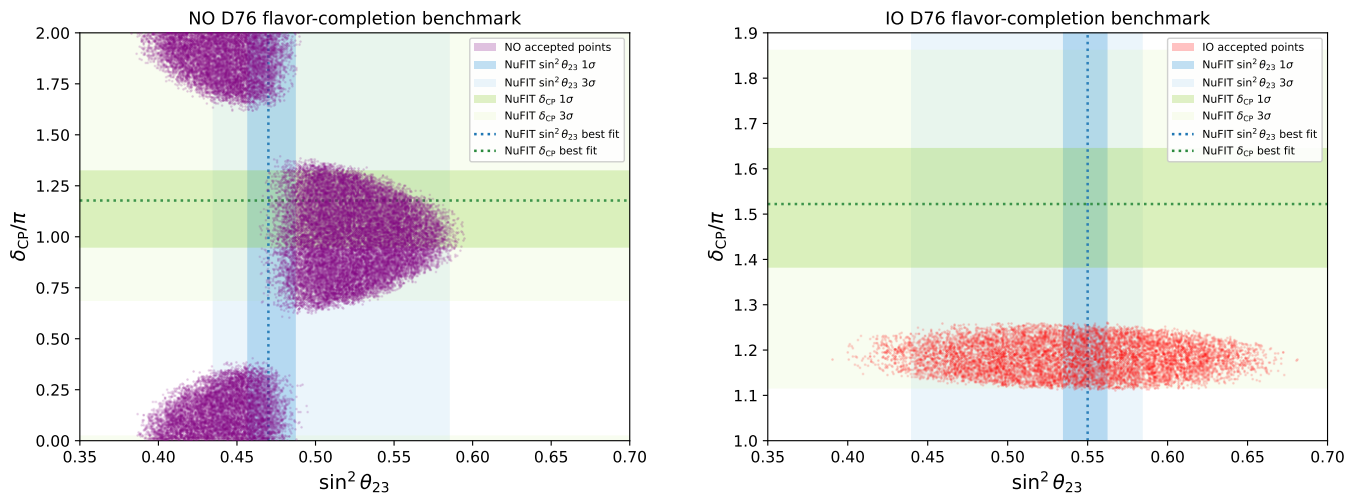


FIG. A3. Fixed flavor+CP benchmark correlations for the  $D_{76}$  texture in the  $(\sin^2 \theta_{23}, \delta_{CP}/\pi)$  plane. The left panel shows an illustrative NO benchmark with  $\theta_R = \pi/21$  and  $\phi_R = \pi$ , while the right panel shows an illustrative IO benchmark with  $\theta_R = \pi/7$  and  $\phi_R = \pi/14$ ; see Fig. A1. The points satisfy the  $D_{76}$  zero condition within numerical tolerance together with the JUNO  $1\sigma$  solar-angle cut. The vertical blue bands and horizontal green bands show the NuFIT  $1\sigma$  and  $3\sigma$  allowed regions for  $\sin^2 \theta_{23}$  and  $\delta_{CP}$ , respectively [98]. The displayed benchmarks are illustrative and not unique; different choices of  $(N, k)$  and  $\phi_R$  can lead to different atmospheric-angle–CP-phase correlations.

The remaining oscillation inputs are scanned over the NuFIT allowed ranges, with the JUNO  $1\sigma$  solar-angle cut imposed. We find that the model prediction for the NO is perfectly within the current NuFIT  $1\sigma$ -allowed range, while for the representative IO benchmark shown here, the allowed region lies outside the current NuFIT  $1\sigma$  preferred region for  $\delta_{CP}$ , but remains within the  $3\sigma$  interval. Of course, these plots are only for illustration purpose; different choices of  $(N, k)$  and  $\phi_R$  can lead to different atmospheric-angle–CP-phase correlations.

The flavor-completion discussion in this Appendix is distinct from the absolute-mass constraints in Fig. 1 in two ways: (i) Fig. 1 is a robust prediction of the massless lightest neutrino scenario, independent of any flavor-specific constructions, unlike the correlation plots shown in this Appendix. The dihedral and flavor+CP conditions constrain the right-handed flavor structure through atmospheric-angle–CP-phase correlations, while Fig. 1 tests the one-massless-neutrino spectrum through  $m_\beta$  and  $\sum_i m_i$ . (ii) Some IO flavor-completion choices can satisfy the oscillation correlation, although the corresponding one-massless-neutrino spectrum is in tension with the DESI  $\Lambda$ CDM mass-sum bound.

- [1] Y. Fukuda *et al.* (Super-Kamiokande), Evidence for oscillation of atmospheric neutrinos, *Phys. Rev. Lett.* **81**, 1562 (1998), [arXiv:hep-ex/9807003](#).
- [2] Q. R. Ahmad *et al.* (SNO), Direct evidence for neutrino flavor transformation from neutral current interactions in the Sudbury Neutrino Observatory, *Phys. Rev. Lett.* **89**, 011301 (2002), [arXiv:nucl-ex/0204008](#).
- [3] P. B. Denton, Neutrino Oscillations in the Three Flavor Paradigm, (2025), [arXiv:2501.08374 \[hep-ph\]](#).
- [4] A. Abusleme *et al.* (JUNO), Sub-percent precision measurement of neutrino oscillation parameters with JUNO, *Chin. Phys. C* **46**, 123001 (2022), [arXiv:2204.13249 \[hep-ex\]](#).
- [5] R. Abbasi *et al.* (IceCube), Measurement of atmospheric neutrino mixing with improved IceCube DeepCore calibration and data processing, *Phys. Rev. D* **108**, 012014 (2023), [arXiv:2304.12236 \[hep-ex\]](#).
- [6] K. Abe *et al.* (Hyper-Kamiokande), Hyper-Kamiokande Design Report, (2018), [arXiv:1805.04163 \[physics.ins-det\]](#).
- [7] B. Abi *et al.* (DUNE), Deep Underground Neutrino Experiment (DUNE), Far Detector Technical Design Report, Volume II: DUNE Physics [10.2172/1599307](#) (2020), [arXiv:2002.03005 \[hep-ex\]](#).
- [8] H. Nunokawa, S. J. Parke, and R. Zukanovich Funchal, Another possible way to determine the neutrino mass hierarchy, *Phys. Rev. D* **72**, 013009 (2005), [arXiv:hep-ph/0503283](#).
- [9] S. Fukasawa, M. Ghosh, and O. Yasuda, Complementarity Between Hyperkamiokande and DUNE in Determining Neutrino Oscillation Parameters, *Nucl. Phys. B* **918**, 337 (2017), [arXiv:1607.03758 \[hep-ph\]](#).
- [10] S. K. Agarwalla, S. Das, A. Giarnetti, D. Meloni, and M. Singh, Enhancing sensitivity to leptonic CP violation using complementarity among DUNE, T2HK, and T2HKK, *Eur. Phys. J. C* **83**, 694 (2023), [arXiv:2211.10620 \[hep-ph\]](#).
- [11] P. B. Denton, M. Friend, M. D. Messier, H. A. Tanaka, S. Böser, J. A. B. Coelho, M. Perrin-Terrin, and T. Stuttard, Snowmass Neutrino Frontier: NF01 Topical Group Report on Three-Flavor Neutrino Oscillations, (2022), [arXiv:2212.00809 \[hep-ph\]](#).

- 
- [1] Y. Fukuda *et al.* (Super-Kamiokande), Evidence for oscillation of atmospheric neutrinos, *Phys. Rev. Lett.* **81**, 1562 (1998), [arXiv:hep-ex/9807003](#).
- [2] Q. R. Ahmad *et al.* (SNO), Direct evidence for neutrino flavor transformation from neutral current interactions in the Sudbury Neutrino Observatory, *Phys. Rev. Lett.*

- [12] S. J. Parke and R. Zukanovich-Funchal, Mass ordering sum rule for the neutrino disappearance channels in T2K, NOvA, and JUNO, *Phys. Rev. D* **111**, 013008 (2025), [arXiv:2404.08733 \[hep-ph\]](#).
- [13] E. Di Valentino, S. Gariazzo, and O. Mena, Neutrinos in Cosmology, (2024), [arXiv:2404.19322 \[astro-ph.CO\]](#).
- [14] J. A. Formaggio, A. L. C. de Gouvêa, and R. G. H. Robertson, Direct Measurements of Neutrino Mass, *Phys. Rept.* **914**, 1 (2021), [arXiv:2102.00594 \[nucl-ex\]](#).
- [15] M. Aker *et al.* (KATRIN), Direct neutrino-mass measurement based on 259 days of KATRIN data, *Science* **388**, adq9592 (2025), [arXiv:2406.13516 \[nucl-ex\]](#).
- [16] G. T. Zatsepin, On the possibility of determining the upper limit of the neutrino mass by means of the flight time, *Pisma Zh. Eksp. Teor. Fiz.* **8**, 333 (1968).
- [17] T. J. Loredo and D. Q. Lamb, Bayesian analysis of neutrinos observed from supernova SN-1987A, *Phys. Rev. D* **65**, 063002 (2002), [arXiv:astro-ph/0107260](#).
- [18] E. Nardi and J. I. Zuluaga, Exploring the sub-eV neutrino mass range with supernova neutrinos, *Phys. Rev. D* **69**, 103002 (2004), [arXiv:astro-ph/0306384](#).
- [19] G. Pagliaroli, F. Rossi-Torres, and F. Vissani, Neutrino mass bound in the standard scenario for supernova electronic antineutrino emission, *Astropart. Phys.* **33**, 287 (2010), [arXiv:1002.3349 \[hep-ph\]](#).
- [20] J.-S. Lu, J. Cao, Y.-F. Li, and S. Zhou, Constraining Absolute Neutrino Masses via Detection of Galactic Supernova Neutrinos at JUNO, *JCAP* **05**, 044, [arXiv:1412.7418 \[hep-ph\]](#).
- [21] R. S. L. Hansen, M. Lindner, and O. Scholer, Timing the neutrino signal of a Galactic supernova, *Phys. Rev. D* **101**, 123018 (2020), [arXiv:1904.11461 \[hep-ph\]](#).
- [22] F. Pompa, F. Capozzi, O. Mena, and M. Sorel, Absolute  $\nu$  Mass Measurement with the DUNE Experiment, *Phys. Rev. Lett.* **129**, 121802 (2022), [arXiv:2203.00024 \[hep-ph\]](#).
- [23] V. Brdar and X.-J. Xu, Timing and multi-channel: novel method for determining the neutrino mass ordering from supernovae, *JCAP* **08**, 067, [arXiv:2204.13135 \[hep-ph\]](#).
- [24] T. Pitik, D. J. Heimsath, A. M. Suliga, and A. B. Balantekin, Exploiting stellar explosion induced by the QCD phase transition in large-scale neutrino detectors, *Phys. Rev. D* **106**, 103007 (2022), [arXiv:2208.14469 \[hep-ph\]](#).
- [25] G. A. Parker and M. Wurm, Constraining the absolute neutrino mass with black hole-forming supernovae and scintillation detectors, *Phys. Rev. D* **109**, 083041 (2024), [arXiv:2311.10682 \[astro-ph.HE\]](#).
- [26] P. B. Denton and Y. Kini, Individual neutrino masses from a supernova, *Phys. Rev. D* **111**, 103006 (2025), [arXiv:2411.13634 \[hep-ph\]](#).
- [27] M. G. Betti *et al.* (PTOLEMY), Neutrino physics with the PTOLEMY project: active neutrino properties and the light sterile case, *JCAP* **07**, 047, [arXiv:1902.05508 \[astro-ph.CO\]](#).
- [28] J. Alvey, M. Escudero, N. Sabti, and T. Schwetz, Cosmic neutrino background detection in large-neutrino-mass cosmologies, *Phys. Rev. D* **105**, 063501 (2022), [arXiv:2111.14870 \[hep-ph\]](#).
- [29] M. Abdul Karim *et al.* (DESI), DESI DR2 results. II. Measurements of baryon acoustic oscillations and cosmological constraints, *Phys. Rev. D* **112**, 083515 (2025), [arXiv:2503.14738 \[astro-ph.CO\]](#).
- [30] Planck Collaboration, N. Aghanim, *et al.*, Planck 2018 results. VI. Cosmological parameters, *Astron. Astrophys.* **641**, A6 (2020), [Erratum: *Astron. Astrophys.* 652, C4 (2021)], [arXiv:1807.06209 \[astro-ph.CO\]](#).
- [31] S. Alam *et al.* (eBOSS), Completed SDSS-IV extended Baryon Oscillation Spectroscopic Survey: Cosmological implications from two decades of spectroscopic surveys at the Apache Point Observatory, *Phys. Rev. D* **103**, 083533 (2021), [arXiv:2007.08991 \[astro-ph.CO\]](#).
- [32] E. Calabrese *et al.* (Atacama Cosmology Telescope), The Atacama Cosmology Telescope: DR6 constraints on extended cosmological models, *JCAP* **11**, 063, [arXiv:2503.14454 \[astro-ph.CO\]](#).
- [33] E. Camphuis *et al.* (SPT-3G), SPT-3G D1: CMB temperature and polarization power spectra and cosmology from 2019 and 2020 observations of the SPT-3G main field, *Phys. Rev. D* **113**, 083504 (2026), [arXiv:2506.20707 \[astro-ph.CO\]](#).
- [34] F. J. Qu *et al.* (ACT, SPT-3G), Unified and Consistent Structure Growth Measurements from Joint ACT, SPT, and Planck CMB Lensing, *Phys. Rev. Lett.* **136**, 021001 (2026), [arXiv:2504.20038 \[astro-ph.CO\]](#).
- [35] F. Couchot, S. Henrot-Versillé, O. Perdereau, S. Plaszczynski, B. Rouillé d'Orfeuil, M. Spinelli, and M. Tristram, Cosmological constraints on the neutrino mass including systematic uncertainties, *Astron. Astrophys.* **606**, A104 (2017), [arXiv:1703.10829 \[astro-ph.CO\]](#).
- [36] E. Abdalla *et al.*, Cosmology intertwined: A review of the particle physics, astrophysics, and cosmology associated with the cosmological tensions and anomalies, *JHEAp* **34**, 49 (2022), [arXiv:2203.06142 \[astro-ph.CO\]](#).
- [37] N. Craig, D. Green, J. Meyers, and S. Rajendran, No  $\nu$ s is Good News, *JHEP* **09**, 097, [arXiv:2405.00836 \[astro-ph.CO\]](#).
- [38] D. Wang, O. Mena, E. Di Valentino, and S. Gariazzo, Updating neutrino mass constraints with background measurements, *Phys. Rev. D* **110**, 103536 (2024), [arXiv:2405.03368 \[astro-ph.CO\]](#).
- [39] I. J. Allali and A. Notari, Neutrino mass bounds from DESI 2024 are relaxed by Planck PR4 and cosmological supernovae, *JCAP* **12**, 020, [arXiv:2406.14554 \[astro-ph.CO\]](#).
- [40] A. Yadav, S. Kumar, C. Kibris, and O. Akarsu,  $\Lambda_s$ CDM cosmology: alleviating major cosmological tensions by predicting standard neutrino properties, *JCAP* **01**, 042, [arXiv:2406.18496 \[astro-ph.CO\]](#).
- [41] D. Green and J. Meyers, Cosmological preference for a negative neutrino mass, *Phys. Rev. D* **111**, 083507 (2025), [arXiv:2407.07878 \[astro-ph.CO\]](#).
- [42] W. Elbers, C. S. Frenk, A. Jenkins, B. Li, and S. Pascoli, Negative neutrino masses as a mirage of dark energy, *Phys. Rev. D* **111**, 063534 (2025), [arXiv:2407.10965 \[astro-ph.CO\]](#).
- [43] D. Naredo-Tuero, M. Escudero, E. Fernández-Martínez, X. Marciano, and V. Poulin, Critical look at the cosmological neutrino mass bound, *Phys. Rev. D* **110**, 123537 (2024), [arXiv:2407.13831 \[astro-ph.CO\]](#).
- [44] J.-Q. Jiang, W. Giarè, S. Gariazzo, M. G. Dainotti, E. Di Valentino, O. Mena, D. Pedrotti, S. S. da Costa, and S. Vagnozzi, Neutrino cosmology after DESI: tightest mass upper limits, preference for the normal ordering, and tension with terrestrial observations, *JCAP* **01**, 153, [arXiv:2407.18047 \[astro-ph.CO\]](#).

- [45] T. Bertólez-Martínez, I. Esteban, R. Hajjar, O. Mena, and J. Salvado, Origin of cosmological neutrino mass bounds: background versus perturbations, *JCAP* **06**, 058, [arXiv:2411.14524 \[astro-ph.CO\]](#).
- [46] G. P. Lynch and L. Knox, What's the matter with  $\Sigma m\nu$ ?, *Phys. Rev. D* **112**, 083543 (2025), [arXiv:2503.14470 \[astro-ph.CO\]](#).
- [47] E. Di Valentino *et al.* (CosmoVerse Network), The CosmoVerse White Paper: Addressing observational tensions in cosmology with systematics and fundamental physics, *Phys. Dark Univ.* **49**, 101965 (2025), [arXiv:2504.01669 \[astro-ph.CO\]](#).
- [48] N. Sailer, G. S. Farren, S. Ferraro, and M. White, Addressing Tensions in  $\Lambda$ CDM Cosmology by an Increase in the Optical Depth to Reionization, *Phys. Rev. Lett.* **136**, 081002 (2026), [arXiv:2504.16932 \[astro-ph.CO\]](#).
- [49] W. Giarè, O. Mena, E. Specogna, and E. Di Valentino, Neutrino mass tension or suppressed growth rate of matter perturbations?, *Phys. Rev. D* **112**, 103520 (2025), [arXiv:2507.01848 \[astro-ph.CO\]](#).
- [50] P. W. Graham, D. Green, and J. Meyers, New interpretations of the cosmological preference for a negative neutrino mass, *Phys. Rev. D* **113**, 043514 (2026), [arXiv:2508.20999 \[astro-ph.CO\]](#).
- [51] A. Cozzumbo, M. Atzori Corona, R. Murgia, M. Archidiacono, and M. Cadeddu, A short blanket for cosmology: the CMB lensing anomaly behind the preference for a negative neutrino mass, (2025), [arXiv:2511.01967 \[astro-ph.CO\]](#).
- [52] J. F. Beacom, N. F. Bell, and S. Dodelson, Neutrinoless universe, *Phys. Rev. Lett.* **93**, 121302 (2004), [arXiv:astro-ph/0404585](#).
- [53] Y. Farzan and S. Hannestad, Neutrinos secretly converting to lighter particles to please both KATRIN and the cosmos, *JCAP* **02**, 058, [arXiv:1510.02201 \[hep-ph\]](#).
- [54] M. Escudero, T. Schwetz, and J. Terol-Calvo, A seesaw model for large neutrino masses in concordance with cosmology, *JHEP* **02**, 142, [Addendum: *JHEP* **06**, 119 (2024)], [arXiv:2211.01729 \[hep-ph\]](#).
- [55] C. Benso, T. Schwetz, and D. Vatsyayan, Large neutrino mass in cosmology and keV sterile neutrino dark matter from a dark sector, *JCAP* **04**, 054, [arXiv:2410.23926 \[hep-ph\]](#).
- [56] A. Das, P. S. B. Dev, C. Gao, S. Ghosh, and T. Kim, Impostor among Neutrinos: Dark Radiation Masquerading as Self-Interacting Neutrinos, *Phys. Rev. Lett.* **136**, 131003 (2026), [arXiv:2506.08085 \[hep-ph\]](#).
- [57] R. K. Sharma, M. Archidiacono, and J. Lesgourgues, Recoupled Dark Radiation reconciling CMB and DESI BAO measurements, (2026), [arXiv:2605.18716 \[astro-ph.CO\]](#).
- [58] L. Boyle, K. Finn, and N. Turok, CPT-Symmetric Universe, *Phys. Rev. Lett.* **121**, 251301 (2018), [arXiv:1803.08928 \[hep-ph\]](#).
- [59] L. Boyle, K. Finn, and N. Turok, The Big Bang, CPT, and neutrino dark matter, *Annals Phys.* **438**, 168767 (2022), [arXiv:1803.08930 \[hep-ph\]](#).
- [60] Z.-j. Tao, Radiative seesaw mechanism at weak scale, *Phys. Rev. D* **54**, 5693 (1996), [arXiv:hep-ph/9603309](#).
- [61] E. Ma, Verifiable radiative seesaw mechanism of neutrino mass and dark matter, *Phys. Rev. D* **73**, 077301 (2006), [arXiv:hep-ph/0601225](#).
- [62] Y. Farzan and E. Ma, Dirac neutrino mass generation from dark matter, *Phys. Rev. D* **86**, 033007 (2012), [arXiv:1204.4890 \[hep-ph\]](#).
- [63] P. Escribano, M. Reig, and A. Vicente, Generalizing the Scotogenic model, *JHEP* **07**, 097, [arXiv:2004.05172 \[hep-ph\]](#).
- [64] P. Minkowski,  $\mu \rightarrow e\gamma$  at a Rate of One Out of  $10^9$  Muon Decays?, *Phys. Lett. B* **67**, 421 (1977).
- [65] R. N. Mohapatra and G. Senjanovic, Neutrino Mass and Spontaneous Parity Nonconservation, *Phys. Rev. Lett.* **44**, 912 (1980).
- [66] M. Gell-Mann, P. Ramond, and R. Slansky, Complex Spinors and Unified Theories, *Conf. Proc. C* **790927**, 315 (1979), [arXiv:1306.4669 \[hep-th\]](#).
- [67] T. Yanagida, Horizontal gauge symmetry and masses of neutrinos, *Conf. Proc. C* **7902131**, 95 (1979).
- [68] A. Y. Smirnov, Seesaw enhancement of lepton mixing, *Phys. Rev. D* **48**, 3264 (1993), [arXiv:hep-ph/9304205](#).
- [69] E. Ma, D. P. Roy, and U. Sarkar, A Seesaw model for atmospheric and solar neutrino oscillations, *Phys. Lett. B* **444**, 391 (1998), [arXiv:hep-ph/9810309](#).
- [70] S. F. King, Large mixing angle MSW and atmospheric neutrinos from single right-handed neutrino dominance and U(1) family symmetry, *Nucl. Phys. B* **576**, 85 (2000), [arXiv:hep-ph/9912492](#).
- [71] L. Lavoura and W. Grimus, Seesaw model with softly broken L(e) - L(muon) - L(tau), *JHEP* **09**, 007, [arXiv:hep-ph/0008020](#).
- [72] S. F. King, Constructing the large mixing angle MNS matrix in seesaw models with right-handed neutrino dominance, *JHEP* **09**, 011, [arXiv:hep-ph/0204360](#).
- [73] P. H. Frampton, S. L. Glashow, and T. Yanagida, Cosmological sign of neutrino CP violation, *Phys. Lett. B* **548**, 119 (2002), [arXiv:hep-ph/0208157](#).
- [74] M. Raidal and A. Strumia, Predictions of the most minimal seesaw model, *Phys. Lett. B* **553**, 72 (2003), [arXiv:hep-ph/0210021](#).
- [75] A. Ibarra and G. G. Ross, Neutrino phenomenology: The Case of two right-handed neutrinos, *Phys. Lett. B* **591**, 285 (2004), [arXiv:hep-ph/0312138](#).
- [76] S. F. King, Littlest Seesaw, *JHEP* **02**, 085, [arXiv:1512.07531 \[hep-ph\]](#).
- [77] R. N. Mohapatra and J. W. F. Valle, Neutrino Mass and Baryon Number Nonconservation in Superstring Models, *Phys. Rev. D* **34**, 1642 (1986).
- [78] M. Malinsky, T. Ohlsson, Z.-z. Xing, and H. Zhang, Non-unitary neutrino mixing and CP violation in the minimal inverse seesaw model, *Phys. Lett. B* **679**, 242 (2009), [arXiv:0905.2889 \[hep-ph\]](#).
- [79] P. S. B. Dev and A. Pilaftsis, Minimal Radiative Neutrino Mass Mechanism for Inverse Seesaw Models, *Phys. Rev. D* **86**, 113001 (2012), [arXiv:1209.4051 \[hep-ph\]](#).
- [80] A. Abada and M. Lucente, Looking for the minimal inverse seesaw realisation, *Nucl. Phys. B* **885**, 651 (2014), [arXiv:1401.1507 \[hep-ph\]](#).
- [81] H. B. Camara, R. G. Felipe, and F. R. Joaquim, Minimal inverse-seesaw mechanism with Abelian flavour symmetries, *JHEP* **05**, 021, [arXiv:2012.04557 \[hep-ph\]](#).
- [82] B. Thapa, S. Barman, S. Bora, and N. K. Francis, A minimal inverse seesaw model with  $S_4$  flavour symmetry, *JHEP* **11**, 154, [arXiv:2305.09306 \[hep-ph\]](#).
- [83] P. H. Frampton, S. L. Glashow, and D. Marfatia, Zeros of the neutrino mass matrix, *Phys. Lett. B* **536**, 79 (2002), [arXiv:hep-ph/0201008](#).
- [84] Z.-z. Xing, Texture zeros and Majorana phases of the neutrino mass matrix, *Phys. Lett. B* **530**, 159 (2002),

- arXiv:hep-ph/0201151.
- [85] P. O. Ludl and W. Grimus, A complete survey of texture zeros in the lepton mass matrices, *JHEP* **07**, 090, [Erratum: *JHEP* 10, 126 (2014)], arXiv:1406.3546 [hep-ph].
- [86] H. Borgohain and D. Borah, Survey of texture zeros with light Dirac neutrinos, *J. Phys. G* **48**, 075005 (2021), arXiv:2007.06249 [hep-ph].
- [87] S. Davidson, G. Isidori, and A. Strumia, The Smallest neutrino mass, *Phys. Lett. B* **646**, 100 (2007), arXiv:hep-ph/0611389.
- [88] H. Fritzsch, Z.-z. Xing, and S. Zhou, Two-zero Textures of the Majorana Neutrino Mass Matrix and Current Experimental Tests, *JHEP* **09**, 083, arXiv:1108.4534 [hep-ph].
- [89] S. Dev, R. R. Gautam, L. Singh, and M. Gupta, Near Maximal Atmospheric Neutrino Mixing in Neutrino Mass Models with Two Texture Zeros, *Phys. Rev. D* **90**, 013021 (2014), arXiv:1405.0566 [hep-ph].
- [90] D. Borah, E. Ma, and D. Nanda, Dark SU(2) gauge symmetry and scotogenic Dirac neutrinos, *Phys. Lett. B* **835**, 137539 (2022), arXiv:2204.13205 [hep-ph].
- [91] D. Borah, E. Ma, and D. Nanda, Dark SU(2)  $\rightarrow$  Z<sub>3</sub>  $\times$  Z<sub>2</sub> gauge symmetry, *Phys. Lett. B* **842**, 137981 (2023), arXiv:2212.11847 [hep-ph].
- [92] E. Witten, An SU(2) Anomaly, *Phys. Lett. B* **117**, 324 (1982).
- [93] B. Pontecorvo, Mesonium and Antimesonium, *Sov. Phys. JETP* **6**, 429 (1958).
- [94] Z. Maki, M. Nakagawa, and S. Sakata, Remarks on the unified model of elementary particles, *Prog. Theor. Phys.* **28**, 870 (1962).
- [95] T. Morozumi, Y. Shimizu, H. Umeeda, and A. Yuu, Hidden relations in three generation seesaw model with Dirac mass matrix of four-zero texture, *Phys. Lett. B* **799**, 135046 (2019), arXiv:1905.11747 [hep-ph].
- [96] S. Dev, S. Kumar, S. Verma, S. Gupta, and R. R. Gautam, Four Zero Texture Fermion Mass Matrices in SO(10) GUT, *Eur. Phys. J. C* **72**, 1940 (2012), arXiv:1203.1403 [hep-ph].
- [97] A. Abusleme *et al.* (JUNO), First measurement of reactor neutrino oscillations at JUNO, (2025), arXiv:2511.14593 [hep-ex].
- [98] I. Esteban, M. C. Gonzalez-Garcia, M. Maltoni, I. Martinez-Soler, J. P. Pinheiro, and T. Schwetz, NuFit-6.0: Updated global analysis of three-flavor neutrino oscillations, *JHEP* **12**, 216, arXiv:2410.05380 [hep-ph].
- [99] A. A. Esfahani *et al.* (Project 8), The Project 8 Neutrino Mass Experiment, in *Snowmass 2021* (2022) arXiv:2203.07349 [nucl-ex].
- [100] G. Drexlin and C. Weinheimer, KATRIN experiment, (2026), arXiv:2601.00248 [nucl-ex].
- [101] F. Adam *et al.* (ECHO), Improved Limit on the Effective Electron Neutrino Mass with the ECHO-1k Experiment, *Phys. Rev. Lett.* **136**, 121801 (2026), arXiv:2509.03423 [hep-ex].
- [102] B. K. Alpert *et al.*, Most Stringent Bound on Electron Neutrino Mass Obtained with a Scalable Low-Temperature Microcalorimeter Array, *Phys. Rev. Lett.* **135**, 141801 (2025), arXiv:2503.19920 [hep-ex].
- [103] A. Font-Ribera, P. McDonald, N. Mostek, B. A. Reid, H.-J. Seo, and A. Slosar, DESI and other dark energy experiments in the era of neutrino mass measurements, *JCAP* **05**, 023, arXiv:1308.4164 [astro-ph.CO].
- [104] P. Ade *et al.* (Simons Observatory), The Simons Observatory: Science goals and forecasts, *JCAP* **02**, 056, arXiv:1808.07445 [astro-ph.CO].
- [105] K. N. Abazajian *et al.* (CMB-S4), *CMB-S4 Science Book, First Edition* (2016) arXiv:1610.02743 [astro-ph.CO].
- [106] T. Brinckmann, D. C. Hooper, M. Archidiacono, J. Lesgourgues, and T. Sprenger, The promising future of a robust cosmological neutrino mass measurement, *JCAP* **01**, 059, arXiv:1808.05955 [astro-ph.CO].
- [107] A. J. Long, C. Lunardini, and E. Sabancilar, Detecting non-relativistic cosmic neutrinos by capture on tritium: phenomenology and physics potential, *JCAP* **08**, 038, arXiv:1405.7654 [hep-ph].
- [108] D. J. Gross and F. Wilczek, Ultraviolet behavior of non-Abelian gauge theories, *Phys. Rev. Lett.* **30**, 1343 (1973).
- [109] H. D. Politzer, Reliable perturbative results for strong interactions?, *Phys. Rev. Lett.* **30**, 1346 (1973).
- [110] J. E. Juknevich, D. Melnikov, and M. J. Strassler, A Pure-Glue Hidden Valley I. States and Decays, *JHEP* **07**, 055, arXiv:0903.0883 [hep-ph].
- [111] T. Hambye and M. H. G. Tytgat, Confined hidden vector dark matter, *Phys. Lett. B* **683**, 39 (2010), arXiv:0907.1007 [hep-ph].
- [112] J. E. Juknevich, Pure-gluon hidden valleys through the Higgs portal, *JHEP* **08**, 121, arXiv:0911.5616 [hep-ph].
- [113] Y. Bai and P. Schwaller, Scale of dark QCD, *Phys. Rev. D* **89**, 063522 (2014), arXiv:1306.4676 [hep-ph].
- [114] K. K. Boddy, J. L. Feng, M. Kaplinghat, and T. M. P. Tait, Self-Interacting Dark Matter from a Non-Abelian Hidden Sector, *Phys. Rev. D* **89**, 115017 (2014), arXiv:1402.3629 [hep-ph].
- [115] K. K. Boddy, J. L. Feng, M. Kaplinghat, Y. Shadmi, and T. M. P. Tait, Strongly interacting dark matter: Self-interactions and keV lines, *Phys. Rev. D* **90**, 095016 (2014), arXiv:1408.6532 [hep-ph].
- [116] N. Yamanaka, S. Fujibayashi, S. Gongyo, and H. Iida, Dark matter in the hidden gauge theory, (2014), arXiv:1411.2172 [hep-ph].
- [117] M. A. Buen-Abad, G. Marques-Tavares, and M. Schmaltz, Non-Abelian dark matter and dark radiation, *Phys. Rev. D* **92**, 023531 (2015), arXiv:1505.03542 [hep-ph].
- [118] A. Soni and Y. Zhang, Hidden SU(N) glueball dark matter, *Phys. Rev. D* **93**, 115025 (2016), arXiv:1602.00714 [hep-ph].
- [119] R. Garani, M. Redi, and A. Tesi, Dark QCD matters, *JHEP* **12**, 139, arXiv:2105.03429 [hep-ph].
- [120] L. Forestell, D. E. Morrissey, and K. Sigurdson, Non-Abelian Dark Forces and the Relic Densities of Dark Glueballs, *Phys. Rev. D* **95**, 015032 (2017), arXiv:1605.08048 [hep-ph].
- [121] L. Forestell, D. E. Morrissey, and K. Sigurdson, Cosmological Bounds on Non-Abelian Dark Forces, *Phys. Rev. D* **97**, 075029 (2018), arXiv:1710.06447 [hep-ph].
- [122] V. De Luca, A. Mitridate, M. Redi, J. Smirnov, and A. Strumia, Colored Dark Matter, *Phys. Rev. D* **97**, 115024 (2018), arXiv:1801.01135 [hep-ph].
- [123] C. J. Morningstar and M. J. Peardon, The Glueball spectrum from an anisotropic lattice study, *Phys. Rev. D* **60**, 034509 (1999), arXiv:hep-lat/9901004.
- [124] B. Lucini, M. Teper, and U. Wenger, Glueballs and k-strings in SU(N) gauge theories: Calculations

- with improved operators, *JHEP* **06**, 012, [arXiv:hep-lat/0404008](#).
- [125] A. A. Anselm and A. A. Johansen, Can electroweak theta term be observable?, *Nucl. Phys. B* **412**, 553 (1994), [arXiv:hep-ph/9305271](#).
- [126] P. Fileviez Perez and H. H. Patel, The electroweak vacuum angle, *Phys. Lett. B* **732**, 241 (2014), [arXiv:1402.6340 \[hep-ph\]](#).
- [127] J. Brister, B. Long, L. Ran, M. Shahzad, Z. Sun, and Y. Zou, Physical remnant of electroweak theta angles, *JHEP* **03**, 205, [arXiv:2510.26281 \[hep-ph\]](#).
- [128] I. Goldman and S. Nussinov, Weakly Interacting Massive Particles and Neutron Stars, *Phys. Rev. D* **40**, 3221 (1989).
- [129] G. Bertone and M. Fairbairn, Compact Stars as Dark Matter Probes, *Phys. Rev. D* **77**, 043515 (2008), [arXiv:0709.1485 \[astro-ph\]](#).
- [130] R. Garani, Y. Genolini, and T. Hambye, New Analysis of Neutron Star Constraints on Asymmetric Dark Matter, *JCAP* **05**, 035, [arXiv:1812.08773 \[hep-ph\]](#).
- [131] G. Busoni, Capture of Dark Matter in Neutron Stars, *Moscow Univ. Phys. Bull.* **77**, 301 (2022), [arXiv:2201.00048 \[hep-ph\]](#).
- [132] M. Baryakhtar, J. Bramante, S. W. Li, T. Linden, and N. Raj, Dark Kinetic Heating of Neutron Stars and An Infrared Window On WIMPs, SIMPs, and Pure Higgsinos, *Phys. Rev. Lett.* **119**, 131801 (2017), [arXiv:1704.01577 \[hep-ph\]](#).
- [133] R. Garani, A. Gupta, and N. Raj, Observing the thermalization of dark matter in neutron stars, *Phys. Rev. D* **103**, 043019 (2021), [arXiv:2009.10728 \[hep-ph\]](#).
- [134] D. Ghosh and A. Das, Probing freeze-in dark matter using Bose-Einstein condensate in neutron star, (2026), [arXiv:2605.22245 \[hep-ph\]](#).
- [135] S. D. McDermott, H.-B. Yu, and K. M. Zurek, Constraints on Scalar Asymmetric Dark Matter from Black Hole Formation in Neutron Stars, *Phys. Rev. D* **85**, 023519 (2012), [arXiv:1103.5472 \[hep-ph\]](#).
- [136] J. Bramante, K. Fukushima, and J. Kumar, Constraints on bosonic dark matter from observation of old neutron stars, *Phys. Rev. D* **87**, 055012 (2013), [arXiv:1301.0036 \[hep-ph\]](#).
- [137] N. F. Bell, A. Melatos, and K. Petraki, Realistic neutron star constraints on bosonic asymmetric dark matter, *Phys. Rev. D* **87**, 123507 (2013), [arXiv:1301.6811 \[hep-ph\]](#).
- [138] B. Dasgupta, R. Laha, and A. Ray, Low Mass Black Holes from Dark Core Collapse, *Phys. Rev. Lett.* **126**, 141105 (2021), [arXiv:2009.01825 \[astro-ph.HE\]](#).
- [139] B. Svetitsky and L. G. Yaffe, Critical Behavior at Finite Temperature Confinement Transitions, *Nucl. Phys. B* **210**, 423 (1982).
- [140] J. Fingberg, U. M. Heller, and F. Karsch, Scaling and asymptotic scaling in the SU(2) gauge theory, *Nucl. Phys. B* **392**, 493 (1993), [arXiv:hep-lat/9208012](#).
- [141] P. Schwaller, Gravitational Waves from a Dark Phase Transition, *Phys. Rev. Lett.* **115**, 181101 (2015), [arXiv:1504.07263 \[hep-ph\]](#).
- [142] A. Soni and Y. Zhang, Gravitational Waves From SU(N) Glueball Dark Matter, *Phys. Lett. B* **771**, 379 (2017), [arXiv:1610.06931 \[hep-ph\]](#).
- [143] C. Caprini *et al.*, Detecting gravitational waves from cosmological phase transitions with LISA: an update, *JCAP* **03**, 024, [arXiv:1910.13125 \[astro-ph.CO\]](#).
- [144] F. Feruglio and A. Romanino, Lepton flavor symmetries, *Rev. Mod. Phys.* **93**, 015007 (2021), [arXiv:1912.06028 \[hep-ph\]](#).
- [145] P. B. Denton and J. Gehrlein, Survey of neutrino flavor predictions and the neutrinoless double beta decay funnel, *Phys. Rev. D* **109**, 055028 (2024), [arXiv:2308.09737 \[hep-ph\]](#).
- [146] G. Chauhan, P. S. B. Dev, I. Dubovyk, B. Dziewit, W. Flieger, K. Grzanka, J. Gluza, B. Karmakar, and S. Zieba, Phenomenology of lepton masses and mixing with discrete flavor symmetries, *Prog. Part. Nucl. Phys.* **138**, 104126 (2024), [arXiv:2310.20681 \[hep-ph\]](#).
- [147] I. de Medeiros Varzielas, M.-S. Liu, A. Sengupta, and J. Talbert, Residual Symmetries and Scalar Multiplet Vacuum Alignment in Non-Abelian Flavour Models, *JHEP* [arXiv:2512.19789 \[hep-ph\]](#).